

## Internal structure of the $T_{cc}(3875)^+$ from its light-quark mass dependence

Michael Abolnikov,<sup>a,\*</sup> Vadim Baru,<sup>a</sup> Evgeny Epelbaum,<sup>a</sup> Arseniy A. Filin,<sup>a</sup>  
Christoph Hanhart<sup>b</sup> and Lu Meng<sup>a</sup>

<sup>a</sup>*Institute of Theoretical Physics II, Ruhr University Bochum,  
Universitätsstraße 150, D-44780 Bochum, Germany*

<sup>b</sup>*Institute for Advanced Simulation (IAS-4), Forschungszentrum Jülich,  
Wilhelm-Johnen-Straße, D-52428 Jülich, Germany*

*E-mail:* [mychaylo.abolnikov@rub.de](mailto:mychaylo.abolnikov@rub.de), [vadimb@tp2.rub.de](mailto:vadimb@tp2.rub.de),  
[evgeny.epelbaum@ruhr-uni-bochum.de](mailto:evgeny.epelbaum@ruhr-uni-bochum.de), [arseniy.filin@ruhr-uni-bochum.de](mailto:arseniy.filin@ruhr-uni-bochum.de),  
[c.hanhart@fz-juelich.de](mailto:c.hanhart@fz-juelich.de), [lu.meng@rub.de](mailto:lu.meng@rub.de)

We employ a chiral effective field theory-based approach to connect  $DD^*$  scattering observables at the physical and variable pion masses accessible in lattice QCD simulations. We incorporate all relevant scales associated with three-body  $DD\pi$  dynamics and the left-hand cut induced by the one-pion exchange for pion masses higher than the physical one, as required by analyticity and unitarity. By adjusting the contact interactions to match experimental data at the physical pion mass and lattice finite-volume energy levels at  $m_\pi = 280$  MeV we predict the trajectory of the  $T_{cc}^+$  pole as a function of the pion mass, finding it consistent with the hadronic-molecule scenario. In particular, we find that the explicit treatment of the one-pion exchange has a pronounced effect on the pole trajectory for  $m_\pi \gtrsim 230$  MeV by pushing the pole into the complex energy plane.

*The 11th International Workshop on Chiral Dynamics (CD2024)  
26-30 August 2024  
Ruhr University Bochum, Germany*

---

\*Speaker

## 1. Introduction

The spectroscopy of exotic hadrons containing heavy quarks has made tremendous progress in recent years, especially concerning the discovery of exotic candidates for multiquark states, as summarized in current reviews [1–8]. One of the most remarkable milestones in the past few years is the discovery of the doubly-charmed exotic state  $T_{cc}^+$  by the LHCb collaboration [9, 10]. Its minimal quark content is  $cc\bar{u}\bar{d}$  and this state is located just a few hundred keV below the  $D^0 D^{*+}$  threshold, having a narrow width which is mainly governed by strong decays to  $DD\pi$ . Studies of  $DD$  mass spectra indicate that  $T_{cc}^+$  is an isoscalar state with spin-parity quantum numbers  $J^P = 1^+$  [10]. The properties of  $T_{cc}^+$  are widely consistent with being a hadronic molecule formed by the residual strong interaction between  $D$  and  $D^*$ . In general, the size of hadronic molecules is controlled by the binding energy and far exceeds that of other multiquark configurations. Due to its weakly bound nature, a spatial extension of the order of 8 fm can be expected for  $T_{cc}^+$ .

The intriguing features of  $T_{cc}^+$  have motivated numerous theoretical studies based on low-energy effective field theories (EFTs) [11–16] and phenomenological models; see, e.g., [7] and references therein. In Ref. [13], special attention was paid to the inclusion of three-body cuts arising from on-shell  $DD\pi$  intermediate states, as a consequence of a consistent treatment of the one-pion exchange (OPE) within a leading-order (LO) chiral EFT expansion. In this work, it has been shown that considering three-body cuts is crucial for an accurate determination of the  $T_{cc}^+$  pole position in the complex energy plane.

In addition to EFT- and model-based works, considerable progress in the study of  $DD^*$  scattering has recently also been achieved in lattice QCD, both employing the Lüscher method [17–20] as well as the HAL QCD approach [21]. However, it has also become clear that the extraction of infinite-volume observables from finite-volume energy levels is challenging in the presence of nearby left-hand cuts arising from long-range interactions such as OPE, as emphasized in, e.g., Ref. [22]. Several extensions of the Lüscher method or alternative approaches have been proposed to overcome this issue [23–26].

In our recent work [27], we emphasize that including the OPE for  $T_{cc}^+$  with a proper treatment of its cuts is needed for theoretical consistency not only at the physical point, as was shown in Ref. [13], but also at unphysically large pion masses. We employ a chiral EFT-based approach to investigate the analytic structure of the scattering amplitude as a function of the pion mass, incorporating all relevant energy and momentum scales as well as the related right- and left-hand cuts from OPE to predict the  $T_{cc}^+$  pole trajectory for pion masses in between  $m_\pi^{\text{ph}}$  and  $3m_\pi^{\text{ph}}$ , where the superscript “ph” indicates the physical pion mass. The acquired information can serve as a benchmark for future lattice QCD calculations and provides additional insights into the internal structure of  $T_{cc}^+$  [28].

## 2. Chiral EFT approach for $DD^*$ scattering

In this work, we focus on the isoscalar channel in connection to the  $T_{cc}^+$  state (for a related study in the isovector channel, we refer to [29]). The long-range interaction between  $D^*$  mesons related to the OPE is incorporated explicitly including all relevant physical scales and related cuts in chiral EFT, consistent with unitarity and analyticity. The a priori unknown short-range interactions are

parametrized using low-energy constants (LECs) which are fixed from both experiment [9, 10] and lattice data at  $m_\pi = 280$  MeV [17]. In between the physical point and the lattice input as well as for  $m_\pi > 280$  MeV, the  $DD^*$  scattering amplitude is obtained by performing chiral extrapolations.

We construct the effective potential  $V$  for  $DD^*$  scattering up to  $\mathcal{O}(Q^2)$  with  $Q = p/\Lambda_b$  in chiral EFT, where  $p \sim m_\pi$  is a characteristic soft momentum scale and  $\Lambda_b$  the breakdown scale of the chiral expansion. The potential is given by a sum of long-range and short-range contributions,

$$V = V_{\text{OPE}}^{(0)} + V_{\text{cont}}^{(0)} + V_{\text{cont}}^{(2)} + \dots \quad (1)$$

Here, effects from the two-pion exchange (TPE) are assumed to be largely saturated by contact terms, as demonstrated in Ref. [30].

All pion mass dependent quantities are expressed as functions of the ratio  $\xi \equiv m_\pi/m_\pi^{\text{ph}}$  — see, e.g., Refs. [31, 32] for explicit expressions of these functions. The  $S$ -wave contact potential is polynomial in the pion mass and momenta, yielding

$$V_{\text{cont}} = V_{\text{cont}}^{(0)} + V_{\text{cont}}^{(2)} = [c_0(\xi) + c_2(\xi)(p_1^2 + p_2'^2)] (\epsilon \cdot \epsilon'^*) \quad (2)$$

for the isoscalar case with  $J^P = 1^+$ , where  $c_0(\xi) = C_0 + D_2(\xi^2 - 1) + \mathcal{O}(\xi^4, p^4)$  and  $c_2(\xi) = C_2 + \mathcal{O}(\xi^2)$  are the pion mass dependent contact terms and  $\mathbf{p}$  ( $\mathbf{p}'$ ),  $\epsilon$  ( $\epsilon'$ ) is the initial (final) momentum and polarization, respectively. The LECs  $C_0$ ,  $C_2$  and  $D_2$  are adjusted to data as described above. We determine  $C_0$  from experimental information, whereas  $C_2$  and  $D_2$  are obtained from lattice input.

The isoscalar OPE potential in the framework of time-ordered perturbation theory (TOPT) is

$$V_{\text{OPE}}(E, \mathbf{p}, \mathbf{p}') = -\frac{g^2}{8f_\pi^2} \frac{(\mathbf{q} \cdot \epsilon)(\mathbf{q} \cdot \epsilon'^*)}{2\omega_\pi(q^2)} [D_1(E, \mathbf{p}, \mathbf{p}') + D_2(E, \mathbf{p}, \mathbf{p}')], \quad (3)$$

with total energy  $E$ , where  $f_\pi$  is the pion decay constant,  $g$  is the coupling constant of pions with heavy mesons and  $\omega_\pi(q^2) = \sqrt{m_\pi^2 + q^2}$  the pion energy. Note that  $f_\pi$ ,  $g$  and the  $D^{(*)}$  masses are also (implicitly) pion mass dependent. Further,  $D_1$  and  $D_2$  are TOPT propagators, given by

$$\begin{aligned} D_1(E, \mathbf{p}, \mathbf{p}') &= \left( 2M_D + \frac{p^2 + p'^2}{2M_D} + \omega_\pi(q^2) - E - i\epsilon \right)^{-1}, \\ D_2(E, \mathbf{p}, \mathbf{p}') &= \left( 2M_{D^*} + \frac{p^2 + p'^2}{2M_{D^*}} + \omega_\pi(q^2) - E - i\epsilon \right)^{-1}. \end{aligned} \quad (4)$$

In this work, we consider the involved mesons in the isospin limit using averaged masses. Contrary to the pion,  $D^{(*)}$  mesons are treated nonrelativistically.

The  $DD^*$  scattering amplitude is obtained by solving the Lippmann-Schwinger equation in the partial wave basis,

$$T_{\alpha\beta}(E, p, p') = V_{\alpha\beta}(E, p, p') + \sum_\gamma \int \frac{d^3q}{(2\pi)^3} V_{\alpha\gamma}(k, q) G(E, q) T_{\gamma\beta}(E, q, p'), \quad (5)$$

where the Greek indices indicate the involved partial waves. A full expression for the  $DD^*$  Green function  $G(E, q)$ , which contains the  $D^*$  self energy as well as the related three-body cut, can be found in Ref. [27] or in the appendix of Ref. [22]. It is of the form

$$G(E, q) = \left[ M_{D^*} + M_D + \frac{q^2}{2\mu} - E - \frac{i}{2}\Gamma(E, q) \right]^{-1}, \quad (6)$$

where  $\mu$  is the reduced mass of the  $DD^*$  system and  $\Gamma(E, q)$  is the dynamic width of the  $D^*$  meson. The dynamic width emerges from resummation of the  $D^*$  self energy,  $D^* \rightarrow D\pi \rightarrow D^*$ , inducing an imaginary part to the  $DD^*$  propagator. The latter corresponds to an intermediate  $DD\pi$  state going on-shell, thus, a three-body cut arises — see Ref. [27] for further details.

### 3. Pion mass dependence of the $T_{cc}^+$ pole position

#### 3.1 LO results

After determining the LECs from experimental data ( $C_0$ ) and lattice information at  $m_\pi = 280$  MeV ( $C_2, D_2$ ), we are able to make predictions for the behavior of the  $T_{cc}^+$  pole as a function of the light-quark mass, or, equivalently, pion mass at next-to-leading-order (NLO). However, it is also informative to consider the LO results, where only  $C_0$  is fixed, without utilizing any lattice input. The related LO pole trajectory shares many common features with the full NLO calculation, such as the behavior close to the physical point and the overall evolution of the state in the complex momentum plane ( $k$ -plane). The qualitative and quantitative similarities between the LO and NLO trajectories indicate the convergence of the chiral expansion and the consistency of our framework.

A common feature of all pole trajectories is that the decay  $DD^* \rightarrow DD\pi$  becomes kinematically forbidden after increasing the pion mass only by about 3% compared to its physical value. Consequently, the  $DD\pi$  intermediate state cannot go on-shell anymore and  $T_{cc}^+$  evolves from a quasi-bound state into a fully bound state. At this point, the analytic structure of the scattering amplitude also changes, since the on-shell  $DD\pi$  cut is replaced by a  $DD^*$  left-hand cut for  $m_\pi \gtrsim 1.03m_\pi^{\text{ph}}$ . By further increasing the pion mass, the pole undergoes a transition from bound to virtual and finally becomes a resonance, as illustrated in Fig. 1. The resulting pole trajectory is consistent with a molecular nature of  $T_{cc}^+$  [28], where going from LO calculation to the NLO affects only the specific pion mass at which the transitions bound  $\rightarrow$  virtual and virtual  $\rightarrow$  resonance occur.

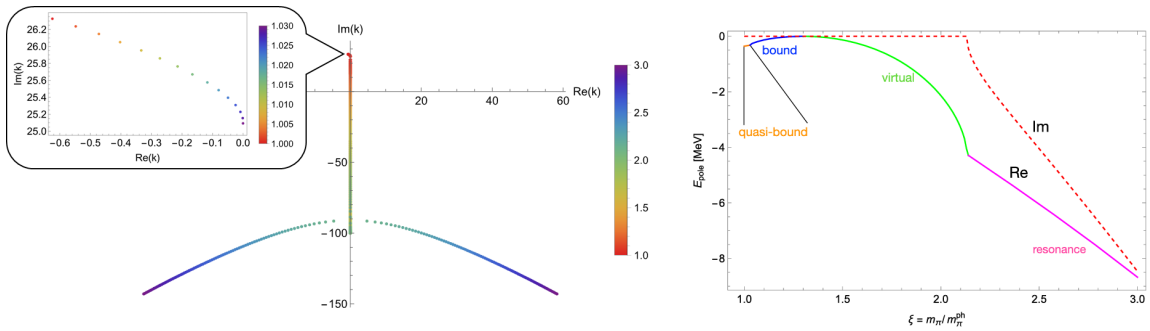


**Figure 1:** Left panel: Pion mass dependence of the  $T_{cc}^+$  pole in the complex  $k$ -plane predicted at LO in chiral EFT. The value of  $\xi$  is indicated by color. The second, more distant virtual state is also shown, along with its collision point with the  $T_{cc}^+$  pole, after which the resonance poles emerge. Right panel: LO trajectory of the  $T_{cc}$  pole in the complex energy plane as a function of  $\xi$ , corresponding to the left panel.  $\text{Re } E_{\text{pole}}$  and  $\text{Im } E_{\text{pole}}$  are shown by solid and dashed lines, respectively. The second, more distant state is not shown; only the energy of the pole with  $\text{Re}(k) > 0$  is shown after the resonance appears.

### 3.2 NLO results

The behavior of the pole changes quantitatively when the higher-order contact terms  $C_2$  and  $D_2$  are included, which are fitted to phase shifts extracted in Ref. [22] from lattice energy levels at  $m_\pi = 280$  MeV [17]. The short-range interaction at NLO in chiral EFT leads to a more repulsive potential. Consequently, the state becomes virtual already at  $m_\pi \simeq 1.25m_\pi^{\text{ph}}$  and evolves into a resonance at  $m_\pi \simeq 1.68m_\pi^{\text{ph}}$ , as shown in Fig. 2. In all cases, the OPE plays a crucial role for the pole trajectory, especially regarding the formation of the  $T_{cc}^+$  as a resonance state. Notably, the latter does not occur in a pure contact theory, such that the state remains virtual. We have also employed a pure contact theory for comparison, leading to a pole trajectory which is in line with the results from Refs. [18, 19], where the OPE is not included, as depicted in Fig. 3. This shows a nontrivial consistency between our and lattice results obtained under the same assumption that the OPE is ignored. On the other hand, our full results demonstrate that the pole trajectory including the OPE changes significantly, yielding a resonance instead of a virtual state.

The uncertainty from cutoff variation is very small and chiral truncation uncertainty is comparable with statistical one — see Ref. [27] for more details on these aspects and other comparisons. Additionally, we note that irreducible TPE contributions are not explicitly included. However, the iterations of the OPE within the dynamical equations already account for the leading effect of the multi-pion left-hand cut (see [33, 34] for related discussions in the context of NN scattering). Furthermore, as demonstrated in Ref. [30], irreducible TPE contributions can be largely saturated by contact terms, which suggests that these terms are suppressed.

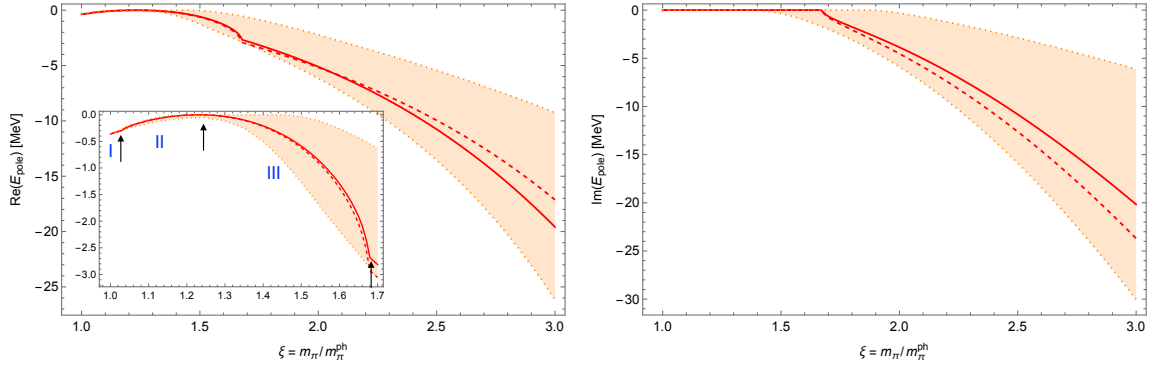


**Figure 2:** The real (left panel) and imaginary (right panel) parts of the  $T_{cc}^+$  pole position at NLO in chiral EFT as a function of the pion mass. The solid red line corresponds to the best fit at NLO with the  $S$ -wave OPE potential, while the orange band stands for the  $1\sigma$  error band estimated using bootstrap. The dashed red line corresponds to the best fit at NLO with the full OPE potential, including  $D$  waves. The inlay highlights the behavior of the pole at lower pion masses, where the transition from quasi-bound (region I) to bound (region II), and then to virtual state occurs (region III), as indicated by the arrows. After  $\xi \approx 1.68$  the  $T_{cc}^+$  becomes a resonance state and the  $\text{Im}$  part of the pole occurs in the right panel.

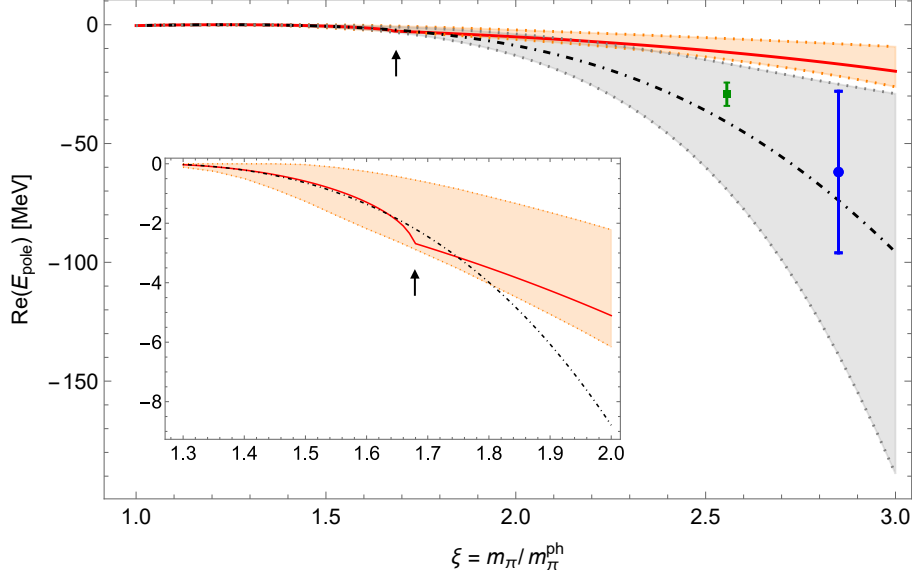


**Figure 3:** Comparison of the  $T_{cc}^+$  pole trajectory at NLO in chiral EFT with that in a pionless (contact) theory (dot-dashed line). The arrow indicates the pion mass ( $\xi \approx 1.68$ ), after which the pole in the pionful theory becomes a resonance state while the pole in the pionless theory remains a virtual state. The blue data point corresponds to a virtual state extracted by the Hadron Spectrum Collaboration at  $m_\pi = 391$  MeV [19], while the green square corresponds to a virtual state at  $m_\pi \approx 348.5$  MeV, extracted using the ERE parameters from Ref. [18].

#### 4. Summary

The pion mass dependence of the  $T_{cc}^+$  pole position is investigated in chiral EFT, where the longest-range interaction is explicitly incorporated by including an OPE potential into the framework and considering the proper analytic structure of the  $DD^*$  scattering amplitude. We parametrize the short-range contributions using one contact term at LO and two more contact terms at NLO in chiral EFT. The resulting  $T_{cc}^+$  pole trajectories are consistent at both orders of the calculation, showing qualitatively the same features, where the pole undergoes a transition from a quasi-bound, to bound, a virtual and finally a resonance state. Notably, the OPE plays an important role for the pole trajectory regarding the last transition, since the formation of a resonance state does not appear in a pure contact theory within the pion mass variation which is considered in this study. The behavior of the  $T_{cc}^+$  pole as a function of the pion mass is in line with a molecular nature of this state.

#### Acknowledgments

This work was supported in part by the MKW NRW under the funding code NW21-024-A, by DFG and NSFC through funds provided to the Sino-German CRC 110 “Symmetries and the Emergence of Structure in QCD” (NSFC Grant No. 11621131001, DFG Project-ID 196253076 -TRR 110), by ERC NuclearTheory (grant No. 885150), by BMBF (Contract No. 05P21PCFP1), and by the EU Horizon 2020 research and innovation programme (STRONG-2020, grant agreement No. 824093).

## References

- [1] A. Esposito, A. Pilloni, and A. D. Polosa, *Multiquark resonances*, [Physics Reports](#) **668**, 1–97 (2017).
- [2] R. F. Lebed, R. E. Mitchell, and E. S. Swanson, *Heavy-quark QCD exotica*, [Prog. Part. Nucl. Phys.](#) **93**, 143–194 (2017).
- [3] F.-K. Guo, C. Hanhart, U.-G. Meißner, Q. Wang, Q. Zhao, and B.-S. Zou, *Hadronic molecules*, [Rev. Mod. Phys.](#) **90**, 015004 (2018).
- [4] Y. Yamaguchi, A. Hosaka, S. Takeuchi, and M. Takizawa, *Heavy hadronic molecules with pion exchange and quark core couplings: a guide for practitioners*, [J. Phys. G](#) **47**, 053001 (2020).
- [5] N. Brambilla, S. Eidelman, C. Hanhart, A. Nefediev, C.-P. Shen, C. E. Thomas, A. Vairo, and C.-Z. Yuan, *The XYZ states: Experimental and theoretical status and perspectives*, [Phys. Rep.](#) **873**, 1–154 (2020).
- [6] F.-K. Guo, X.-H. Liu, and S. Sakai, *Threshold cusps and triangle singularities in hadronic reactions*, [Prog. Part. Nucl. Phys.](#) **112**, 103757 (2020).
- [7] H.-X. Chen, W. Chen, X. Liu, Y.-R. Liu, and S.-L. Zhu, *An updated review of the new hadron states*, [Rep. Prog. Phys.](#) **86**, 026201 (2023).
- [8] L. Meng, B. Wang, G.-J. Wang, and S.-L. Zhu, *Chiral perturbation theory for heavy hadrons and chiral effective field theory for heavy hadronic molecules*, [Phys. Rep.](#) **1019**, 1–149 (2023).
- [9] R. Aaij et al. (LHCb Collaboration), *Observation of an exotic narrow doubly charmed tetraquark*, [Nat. Phys.](#) **18**, 751–754 (2022).
- [10] R. Aaij et al. (LHCb Collaboration), *Study of the doubly charmed tetraquark  $T_{cc}^+$* , [Nat. Commun.](#) **13**, 3351 (2022).
- [11] M. Albaladejo,  *$T_{cc}^+$  coupled channel analysis and predictions*, [Phys. Lett. B](#) **829**, 137052 (2022).
- [12] L. Meng, G.-J. Wang, B. Wang, and S.-L. Zhu, *Probing the long-range structure of the  $T_{cc}^+$  with the strong and electromagnetic decays*, [Phys. Rev. D](#) **104**, L051502 (2021).
- [13] M.-L. Du, V. Baru, X.-K. Dong, A. Filin, F.-K. Guo, C. Hanhart, A. Nefediev, J. Nieves, and Q. Wang, *Coupled-channel approach to  $T_{cc}^+$  including three-body effects*, [Phys. Rev. D](#) **105**, 014024 (2022).
- [14] E. Braaten, L.-P. He, K. Ingles, and J. Jiang, *Triangle singularity in the production of  $T_{cc}^+(3875)$  and a soft pion*, [Phys. Rev. D](#) **106**, 034033 (2022).
- [15] B. Wang and L. Meng, *Revisiting the  $DD^*$  chiral interactions with the local momentum-space regularization up to the third order and the nature of  $T_{cc}^+$* , [Phys. Rev. D](#) **107**, 094002 (2023).
- [16] L. Dai, S. Fleming, R. Hodges, and T. Mehen, *Strong decays of  $T_{cc}^+$  at NLO in an effective field theory*, [Phys. Rev. D](#) **107**, 076001 (2023).
- [17] M. Padmanath and S. Prelovsek, *Signature of a Doubly Charm Tetraquark Pole in  $DD^*$  Scattering on the Lattice*, [Phys. Rev. Lett.](#) **129**, 032002 (2022).

- [18] S. Chen, C. Shi, Y. Chen, M. Gong, Z. Liu, W. Sun, and R. Zhang,  $T_{cc}^+(3875)$  relevant  $DD^*$  scattering from  $N_f = 2$  lattice QCD, *Phys. Lett. B* **833**, 137391 (2022).
- [19] T. Whyte, D. J. Wilson, and C. E. Thomas, Near-threshold states in coupled  $DD^* - D^*D^*$  scattering from lattice QCD, *arXiv:2405.15741* (2024).
- [20] S. Collins, A. Nefediev, M. Padmanath, and S. Prelovsek, Toward the quark mass dependence of  $T_{cc}^+$  from lattice QCD, *Phys. Rev. D* **109**, 094509 (2024).
- [21] Y. Lyu, S. Aoki, T. Doi, T. Hatsuda, Y. Ikeda, and J. Meng, Doubly Charmed Tetraquark  $T_{cc}^+$  from Lattice QCD near Physical Point, *Phys. Rev. Lett.* **131**, 161901 (2023).
- [22] M.-L. Du, A. Filin, V. Baru, X.-K. Dong, E. Epelbaum, F.-K. Guo, C. Hanhart, A. Nefediev, J. Nieves, and Q. Wang, Role of Left-Hand Cut Contributions on Pole Extractions from Lattice Data: Case Study for  $T_{cc}(3875)^+$ , *Phys. Rev. Lett.* **131**, 131903 (2023).
- [23] A. Baião Raposo and M. T. Hansen, Finite-volume scattering on the left-hand cut, *JHEP* **2024**, 75 (2024).
- [24] L. Meng, V. Baru, E. Epelbaum, A. A. Filin, and A. M. Gasparian, Solving the left-hand cut problem in lattice QCD:  $T_{cc}(3875)^+$  from finite volume energy levels, *Phys. Rev. D* **109**, L071506 (2024).
- [25] R. Bubna, H.-W. Hammer, F. Müller, J.-Y. Pang, A. Rusetsky, and J.-J. Wu, Lüscher equation with long-range forces, *JHEP* **2024**, 168 (2024).
- [26] M. T. Hansen, F. Romero-López, and S. R. Sharpe, Incorporating  $DD\pi$  effects and left-hand cuts in lattice QCD studies of the  $T_{cc}(3875)^+$ , *JHEP* **2024**, 51 (2024).
- [27] M. Abolnikov, V. Baru, E. Epelbaum, A. A. Filin, C. Hanhart, and L. Meng, Internal structure of the  $T_{cc}(3875)^+$  from its light-quark mass dependence, *Phys. Lett. B* **860**, 139188 (2025).
- [28] I. Matuschek, V. Baru, F.-K. Guo, and C. Hanhart, On the nature of near-threshold bound and virtual states, *Eur. Phys. J. A* **57**, 101 (2021).
- [29] L. Meng, E. Ortiz-Pacheco, V. Baru, E. Epelbaum, M. Padmanath, and S. Prelovsek, Doubly charm tetraquark channel with isospin 1 from lattice QCD, *Phys. Rev. D* **111**, 034509 (2025).
- [30] J. T. Chacko, V. Baru, C. Hanhart, and S. L. Krug, Two-pion exchange for coupled-channel heavy-meson heavy-(anti) meson scattering, *arXiv:2411.13303* (2024).
- [31] V. Baru, E. Epelbaum, A. Filin, C. Hanhart, U.-G. Meißner, and A. Nefediev, Quark mass dependence of the  $X(3872)$  binding energy, *Phys. Lett. B* **726**, 537–543 (2013).
- [32] V. Baru, E. Epelbaum, A. A. Filin, J. Gegelia, and A. V. Nefediev, Binding energy of the  $X(3872)$  at unphysical pion masses, *Phys. Rev. D* **92**, 114016 (2015).
- [33] V. Baru, E. Epelbaum, A. A. Filin, and J. Gegelia, Low-energy theorems for nucleon-nucleon scattering at unphysical pion masses, *Phys. Rev. C* **92**, 014001 (2015).
- [34] V. Baru, E. Epelbaum, and A. A. Filin, Low-energy theorems for nucleon-nucleon scattering at  $M_\pi = 450$  MeV, *Phys. Rev. C* **94**, 014001 (2016).